Available online at www.eccomasproceedia.org
Eccomas Proceedia COMPDYN (2025) 646- 656

ECCOMAS
Proceedia

COMPDYN 2025
10th ECCOMAS Thematic Conference on
Computational Methods in Structural Dynamics and Earthquake Engineering
M. Papadrakakis, M. Fragiadakis (eds.)
Rhodes Island, Greece, 15-18 June 2025

ENHANCED PERFORMANCE-BASED SEISMIC DESIGN TOWARD FUNCTIONAL RECOVERY ACHIEVEMENT OF STEEL BUILDINGS

Lizhu Chen[1], Shuaikang Wang[2], Lucia Tirca[3]

[1]Concordia University
1455 Boulevard de Maisonneuve O., Montreal, QC, H3G 1M8, Canada
jackacie@gmail.com

[2]Concordia University
1455 Boulevard de Maisonneuve O., Montreal, QC, H3G 1M8, Canada
shuaikang0623@gmail.com

[3]Concordia University
1455 Boulevard de Maisonneuve O., Montreal, QC, H3G 1M8, Canada
Lucia.Tirca@concordia.ca

Abstract

Current building codes are prescriptive in nature and primarily focus on ensuring life safety during seismic events, often neglecting the broader objective of functional recovery. While the FEMA P-58 methodology provides a comprehensive performance-based seismic design, it lacks design criteria tailored to functional recovery. The main objective of this paper is to present the innovative Strongback Braced Frame as a candidate able to assure seismic functional recovery and demonstrate through case studies the system efficiency against the traditional Concentrically Braced Frame (CBF) under short and long duration ground motions. Nonlinear time-history analyses using OpenSees reveal the feasibility of SBF in high-risk seismic regions. The findings resulted from case studies provide practitioners comparative behavioral characteristics of SBF versus MD-CBF in terms of interstorey drift, residual interstorey drift and floor acceleration. It is worth mentioning that higher-mode forces developed in SBF are not limited by the yield mechanism of ductile system but by ground motion intensity, which implies large inertial effects relative to first-mode response. However, forces in the first mode are limited by the global mechanism.

Keywords: Performance-based seismic design, functional recovery, strongback braced frame

ISSN:2623-3347
Peer-review under responsibility of the organizing committee of COMPDYN 2025.
doi: 10.7712/120125.12680.25504

1 INTRODUCTION

The current building codes are prescriptive in nature and developed to provide building's safety under earthquake events. Although the most comprehensive performance-based seismic design (PBSD) methodology was released in FEMA P-58-1[1], appropriate design criteria for practitioners are not currently available. According to FEMA P-58, the performance measures include direct economic losses (building repair or replacement cost) and indirect losses as recovery time, which consists of mobilization time and repair time. To assess the building repair cost, the Performance Assessment Calculation Tool (PACT) provided in FEMA P-58-3 [2] yields an appropriate estimate of repair cost, while for the repair time the fault three analysis is suggested [3]. It is worth mentioning that PACT [2] yields a crude estimate of repair time, and the REDI^{TM} downtime model [4] is based on a fixed repaired schedule and a predetermined workforce, while the mobilization time is based on the damage state of the most severely damaged component. It is noted that PACT possesses a library with more than 700 fragility and consequence data for members and connections of most common seismic force resisting systems (SFRSs) and nonstructural components. Typically, peak storey drift or peak floor acceleration parameters are used to determine the damaged components. In addition, a collapse fragility function expressing the probability of building collapse and a residual drift function are also required. It is noted that residual drift is a measure of building's repairability criteria.

Although the PBSD methodology shows advances towards measuring the building performance, is still founded on safety-based objectives rather than recovery-based objectives that are focused on identification of needed functions and services in the aftermath of an earthquake event. At present, there are neither prescriptions available for strength, stiffness, or capacity of members/ components of a traditional seismic force resistant system (SFRS), nor definition of innovative SFRSs that could assure functional recovery of a building within a certain time [5]. The determination of recovery time under a given intensity earthquake associated with recovery-based objectives is the key for recovery-based design. After an earthquake event, the proposed recovery trajectories are: (i) assure building stability for allowing building inspection, (ii) provide structural recovery for shelter-in-place condition, (iii) conduct retrofit for re-occupancy, and (iv) functional recovery. Time to recovery of function can be considered as short, intermediate, and long term. To an extent, the type of building importance category defined in [6] is associated with functional recovery category (FRC) which is labelled in [5] from "A" to "D", where FRC-A is for post-disaster buildings and FRC-D for other buildings excluding schools, condominium, critical retail and critical business enterprises. Under 2%/50 years design spectrum [6, 7], the target functional recovery time recommended in [5] varies from hours for FRC-A, from weeks to months for FRC-C and months to years for FRC-D, respectively. Further, different target recovery time that varies based on earthquake hazard levels (from 10%/50 years to 2%/ 50 years and beyond) could be established.

The main objective of this paper is to present the innovative Strongback Braced Frame (SBF) system as a candidate able to mitigate the soft-storey response and assure seismic functional recovery when the variant with "damage-free" braces is used. This is demonstrated through case studies subjected to short and long duration ground motions. A comparison with the seismic response of traditional Concentrically Braced Frame (CBF) is also presented.

2 STRONGBACK BRACED FRAME

The Strongback Braced Frame (SBF) with buckling braces is derived from the traditional CBF. The ductile response of SBF is provided by yielding of ductile braces, while the elastic vertical truss (strongback) installed interior or exterior to braced frame is able to sustain the system's deformation even after one ductile brace exhibited fracture caused by low-cycle fatigue. However, the vertical elastic truss (SB) generates higher modes contributions that cannot be captured using the traditional capacity design approach.

2.1 Higher modes effect

To estimate the force demand in structural systems that includes inertial forces triggered by higher modes, Chopra et al. [8] introduced the Modified Modal Pushover Analysis (MMPA). Thus, the MMPA assumes the seismic force-resisting system (SFRS) to be linearly elastic and accounts on the seismic demand due to higher modes. The method is designed to be used alongside a design spectrum for building location, as required by the building code. The force distribution and target displacement in MMPA are based on two key assumptions: (i) the first vibration mode governs the structural response, and (ii) the mode shape remains unchanged after the members of ductile system yield, while assuming negligible the coupling of elastic modes upon the initiation of inelastic behavior.

To simplify the estimation of higher mode contributions in design, in [9] it was proposed to use the MMPA procedure with a truncated response spectrum analysis (RSA). Following this approach, the response due to the first mode (r_1) is calculated assuming that the system behaves in the inelastic range, while the contributions of higher modes ($r_2 \ldots r_n$) are computed considering the system in the elastic range. Then, the total response (r) is determined from Eq. (1).

$$r = r_g + \left|r_{1,pl}\right| + \sqrt{r_{2,el}^2 + r_{3,el}^2 + \cdots + r_{n,el}^2} \tag{1}$$

Herein, r_g represents the contribution of gravity component of seismic load combination case. Notably, the yielding members of SBF do not restrain the higher mode contributions to storey shear and floor acceleration. As the influence of higher modes increases with building height, the resulting forces can lead to impractical proportioning of the strongback system. To address this issue and mitigate storey shear demand in high-rise buildings, the segmental (modular) elastic spine system was proposed in [10]. More recently, for estimating forces in SBFs, the Generalized Modified Modal Superposition Procedure (GMMSP) was proposed in [11]. While the GMMSP offers a promising approach, it is not evaluated in this study.

2.2 Design procedure

The design procedure for SBF follows Eq. (1) and a visual representation of Eq. (1) applied to SBF is depicted in Fig. 1. The design procedure is outlined below.

(1) Designing the primary ductile system (e.g. CBF):
- Use the Equivalent Static Force Procedure (ESFP) required by building code and design braces of traditional CBF as per [12]. The CBF is proportioned to resist 100% base shear.
- Apply capacity design to size the beams and columns of CBF (primary system) according with [12]. It is noted that the CBF column supporting the Strongback shall be continuous.

(2) Estimating the Strongback (SB) members:
- Compute the ductile brace member forces assuming the formation of a full plastic mechanism in the first mode (Fig. 1a).
- Consider equilibrium of forces to compute the axial forces transferred from the primary system into SB members and estimate its preliminary sections.

(3) Conducting preliminary design of SBF:
- Develop a numerical model by using member sections resulted for the primary ductile system in Step 1 and member sections for SB truss from Step 2. Then, perform an Eigenvalue analysis to determine the elastic natural periods and mode shapes of structure.

(4) Assessing the higher modes contribution for SB design:

- To account for higher modes contribution, employ a truncated elastic design spectrum as illustrated in Fig. 2.
- Compute independently the storey forces associated with the 2nd and 3rd mode, as exemplified in Figs. 1b and 1c.
- Compute the higher mode forces induced in the SB truss members using the Square Root of the Sum of Squares (SRSS) combination rule as per Eq. (1).

(5) Computing the response of SBF and estimating the feasibility of design method:
- Using member sections resulted for primary ductile system in Step 1 and the re-designed truss member sections from Step 4, calculate the total response according to Eq. (1).
- Verify member sections against nonlinear dynamic analysis. This step ensures that the proposed design method meets the expected nonlinear responses of SBF under ground motions.

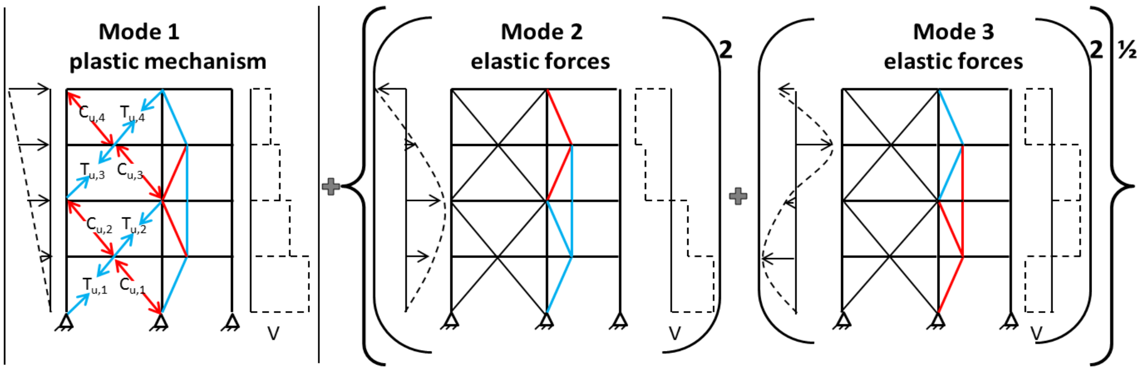

Fig. 1: Graphical illustration of computation method for 4-storey SBF, adapted from [9].

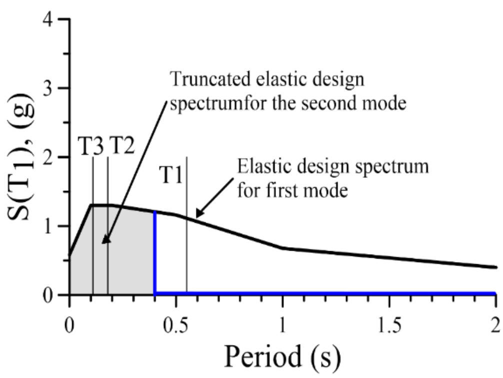

Fig. 2: Elastic design spectrum and the truncated elastic design spectrum for 2nd mode (shaded area) for Victoria.

3 CASE STUDY

The case study is a 4-storey office building located on Site Class C in Victoria, B.C., Canada. For comparison purposes, the building is designed considering two SFRSs: (a) the traditional Moderately-Ductile Concentrically Braced Frame (MD-CBF), and (b) the innovative SBF with exterior SB. The same building plan is used for MD-CBF and SBF and is plotted in Fig. 3a.

3.1 Design of MD-CBF and SBF

Both MD-CBF and SBF were designed in accordance with the building code [7] and the steel design standard [12]. For Victoria, Site class C, the spectral ordinates at 0, 0.1, 0.2, 0.5, 1.0 and 2.0 s are 0.58, 1.3, 1.3, 1.16, 0.676 and 0.399 g and the elastic design spectrum is illustrated in Fig. 2. Using the ESFP, the base shear is:

$$V = I_E S(T_a) M_v W / R_d R_0 \tag{2}$$

where I_E is the importance factor (I_E =1.0), M_v is the effect of higher modes on base shear (M_v=1), T_a = 0.025h_n is the fundamental period where h_n =14.8 m is the building height, W = 29457 kN is the seismic weight, and R_dR_0 =3x1.3 are the ductility and overstrength reduction factors, respectively. In accordance with [7], when dynamic analysis is employed, T_a can be amplified by a factor of 2 which leads to T_a = 0.74 s and $S(T_a)$= 0.93g. From Eq. (2) results V = 7007 kN, but V cannot be larger than V_{max} calculated as:

$$V_{max} = max\ (2/3 I_E S(0.2) M_v W/R_d R_0;\ I_E S(0.5) M_v W/R_d R_0) \tag{3}$$

From Eq. (3) results V_{max} = 8762 kN which is larger than V; hence, V is used in design. In addition, the notional lateral loads, V_N, computed as 0.005 times the factored gravity loads $\sum C_{(D+0.5L+0.25S)}$ contributed to each floor and the P-delta effect were considered, while the torsional effect was neglected. All ductile braces, as well as those of SB are made of hollow structural sections (HSS) and all beams and columns are made of I-shaped. For HSS members, the yield strength (F_y) is 350 MPa and the probable yield stress R_yF_y is 460 MPa. For I-shaped members F_y is 345 MPa. To design members of MD-CBF beams and columns the capacity design approach was applied. Using data from preliminary design (ESFP), the three-dimensional building model was developed in ETABS and subjected to dynamic analysis by means of RSA. The resulted base shear, V_{dyn} =8477 kN, is larger than V computed with Eq. (2) and all member sections were verified and provided in Fig. 4a. From Eigenvalue analysis in N-S direction, the first mode period for MD-CBF building resulted T_1 = 0.551 s and the second and third mode period are provided in Table 1.

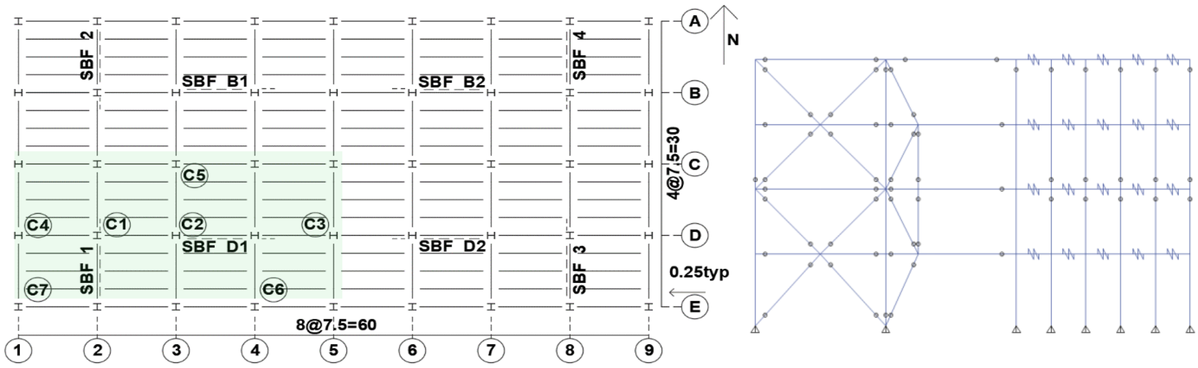

Fig. 3: Plan view of 4-storey SBF building (a) and the OpenSees model of ¼ of building floor plan (b).

Type	ETABS			OpenSees		
	T_1 (s)	T_2 (s)	T_3 (s)	T_1 (s)	T_2 (s)	T_3 (s)
MD-CBF	0.551	0.201	0.125	0.554	0.205	0.138
SBF	0.520	0.169	0.102	0.522	0.171	0.105

Table 1: Periods of CBF, SBF resulted from eigenvalue analysis.

The SBF system was designed using the methodology outlined in Section 2. The same R_dR_0 value as per MD-CBF was considered. From Eigenvalue analysis in N-S direction, the first mode period for SBF building is T_1 = 0.52 s (Table 1), which is slightly lower than T_1 for MD-CBF. Member sizes for the SBF are provided in Fig. 4(b). It is noted that larger column sections are required for column attached to SB. However, the same sections were used for both columns of primary system. The ratio between the storey stiffness associated with braces and ties of SB truss and that of ductile braces of SBF is on average 1.96 with a peak value of 2.68 at the 4th floor. If the SB truss is placed interior to the braced frame, this ratio would increase to an average of 4, which is consistent with findings in [13, 14].

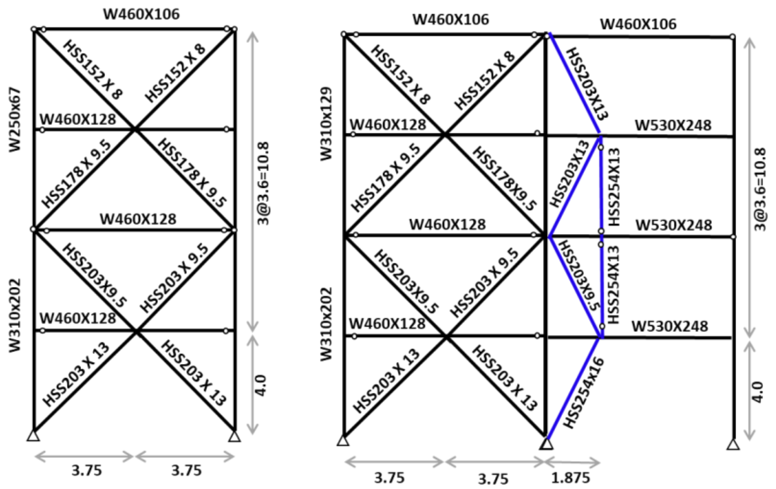

(a) (b)

Fig. 4: Summary of member sections for: a) MD-CBF, and b) SBF.

3.2 Numerical modelling in OpenSees

Due to building symmetry, only one-quarter of floor plan braced in the N-S direction by SBF 1 (Fig. 3a) was modelled using a two-dimensional (2D) numerical model (Fig. 3b) developed in OpenSees. To simulate the out-of-plane buckling of HSS braces, six degrees of freedom were considered in the 2D model. Each HSS brace was discretized into 16 nonlinear beam-column elements with distributed plasticity and fiber-based sections, using four integration points per element. An initial out-of-straightness of $L_{brace}/500$ was assigned to all ductile braces in the out-of-plane direction. The *Steel02* material with the yield strength set to the probable yield stress (R_yF_y=460 MPa) was assigned to HSS braces and a low-cycle fatigue material model with parameters proposed in [15] was wrapped around the *Steel02* material in order to capture brace fracture. The same modeling approach was used for HSS members of SB truss. I-shaped beams and columns were modeled using nonlinear beam-column elements with distributed plasticity and fiber-based sections. A 2% Rayleigh damping, proportional to mass and stiffness and computed for the 1st and 3rd modes, was assigned to elastic members. The rigid diaphragm effect was accounted for using the *equalDOF* command in OpenSees. The mode periods obtained from OpenSees are also provided in Table 1.

3.3 Ground motion selection and scaling

Given the proximity of Victoria, B.C., to Cascadia subduction fault zone, the seismic hazard incorporates both crustal and subduction zone ground motions (GMs). For this study, crustal GMs were selected from the Northridge (M_w = 6.7) and Loma Prieta (M_w = 6.9) earthquake events, while subduction GMs were sourced from the megathrust (M_w = 9) Tohoku earthquake in Japan (2011). Two suites of ground motions comprising 7 crustal (marked from #C1 to #C7) and 7 subduction (marked from #S1 to #S7) records were compiled and scaled to match the 2%/50-year design spectrum for Victoria over the periods of interest $0.15T_1$ - $2.0T_1$, specified in [7]. These GMs can be found in [16]. The response spectra of scaled crustal and subduction GMs, along with their mean response spectrum and the design spectrum associated with 2%/50 yrs. as per [7], are plotted in Figs. 6a and 6b, respectively. The scaling process ensured that the mean response spectrum of each suite matches or is above the design spectrum over the period of interest $0.15T_1$-$2.0T_1$. For discussion purposses, the 10%/50 yrs., 5%/10 yrs., and 2%/50 yrs. spectra associated with the 2020 NBC provisions [6] are also provided. As depicted, the 2%/50 yrs. design spectrum associated with [7] matches closely the 5%/50 yrs. spectrum given in [6].

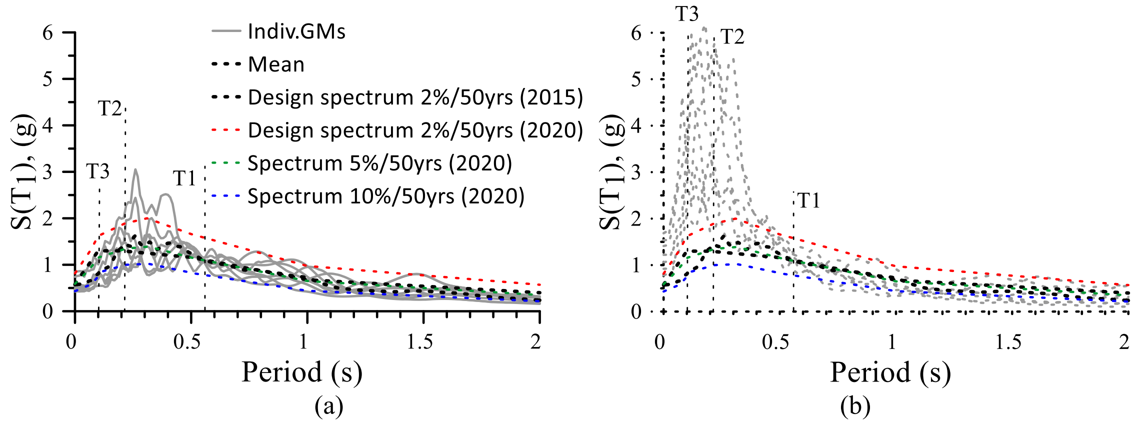

Fig. 5: Design spectrum for Victoria, Site Class C as per [7], alongside with scaled response acceleration spectrum of individual GMs and their mean: a) crustal GM suite and b) subduction GM suite.

3.4 Nonlinear time-history analysis

Nonlinear time-history analyses were conducted using the 2D numerical model developed in OpenSees. Both MD-CBF and SBF building models were subjected to scaled crustal and subduction zone GMs according with [7], and key response parameters such as interstorey drift (ISD), residual drift (RISD), floor acceleration (FA), and shear forces were recorded. These parameters, resulted under GMs scaled at design level (D.L.) as per [7], are presented in Fig. 6.

Under crustal GMs, the SBF demonstrates uniform distribution of ISDs along the building height; hence, when comparing with MD-CBF, the SBF is able to diminish the peak ISDs especially under GMs #C1 and #C6. Additionally, the SBF is able to maintain RISD below 0.25% h_s, where h_s is the storey height. However, SBFs exhibited increased FAs especially under #C2 and #C4 records. In general, under 3 out of 7 crustal GMs the FA is between 1.0g and 1.5g.

Under subduction zone GMs scaled at D.L., the SBF is able to mitigate the concentration of damage at top floor. For example, under GMs #S3 - #S5, the peak ISD decreased in average by 50% when comparing to MD-CBF. While the reduction in RISD was less pronounced due to already low values in both systems, the SBF system exhibited smoother floor acceleration (FA) distribution across the building height. However, under 3 out of 7 subduction GMs, the peak FA is between 1.5 g and 2.0 g. This improvement in terms of ISD and RISD reduces the potential for damage to drift-sensitive nonstructural components, but the acceleration-sensitive nonstructural components will exhibit various levels of damage.

Green lines in Fig. 7 present the mean of ISD, RISD, and FA, computed from data presented in Fig. 6 which is associated to 2%/50 yrs. hazard as per [7]. It is worth mentioning that the 2%/50 yrs. hazard defined in [6] is about 50% greater than that provided in [7]. Red lines in Fig. 7 present the mean of ISD, RISD, and FA under crustal and subduction GMs scaled for 2%/50 yrs. design spectrum in [6]. Thus, the peak of mean ISD and RISD of MD-CBF increase under crustal GMs to 1.1%h_s and 0.12%h_s, respectively. Under subduction GMs, the response of MD-CBF is similar. However, for MD-CBF the peak of mean FA under crustal GMs occurred at top floor (1.1g) and that under subduction GMs at bottom floor (1.8 g), which shows 50% increase. Comparing to MD-CBF, a decrease in peak ISD and RISD occurred for SBF, but no changes in FA were observed. Analysing data from Fig. 7 is concluded that increasing the demand from S(T_1)=1.11g [7] to S(T_1) =1.6g [6] light damage of drift-sensitive nonstructural components may occur for both SBF and MD-CBF under crustal and subduction GMs, while significant damage can be exhibited by acceleration-sensitive nonstructural components under subduction zone GMs.

As plotted in Fig. 5, the 5%/50 yrs. design spectrum associated with the NBC 2020 [6] almost overlaps with 2%/50 yrs. design spectrum associated with the NBC 2015 [7].

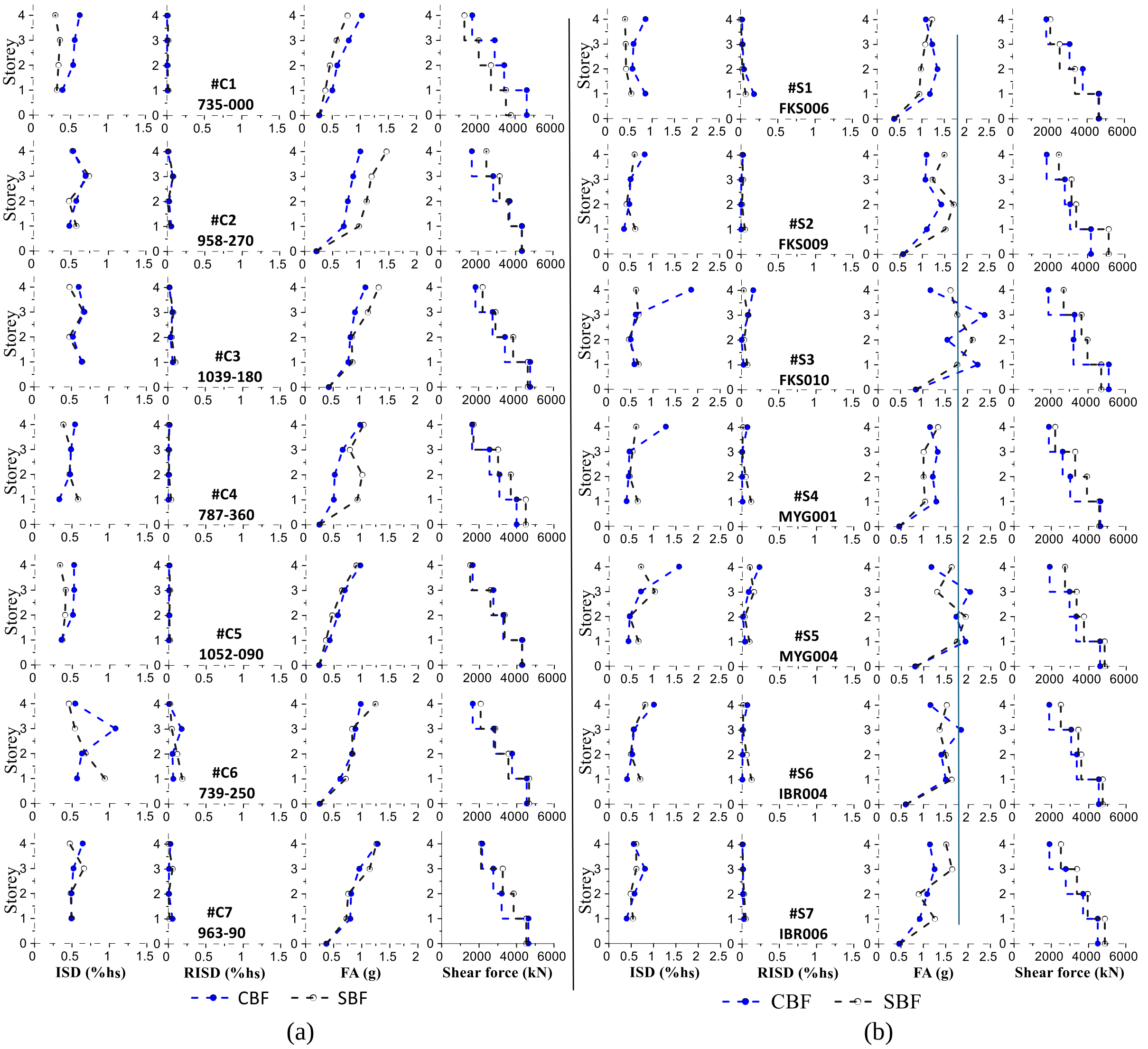

Fig. 6: Nonlinear responses of 4-storey CBF and SBF buildings subjected to (a) crustal GMs and (b) scaled at DL.

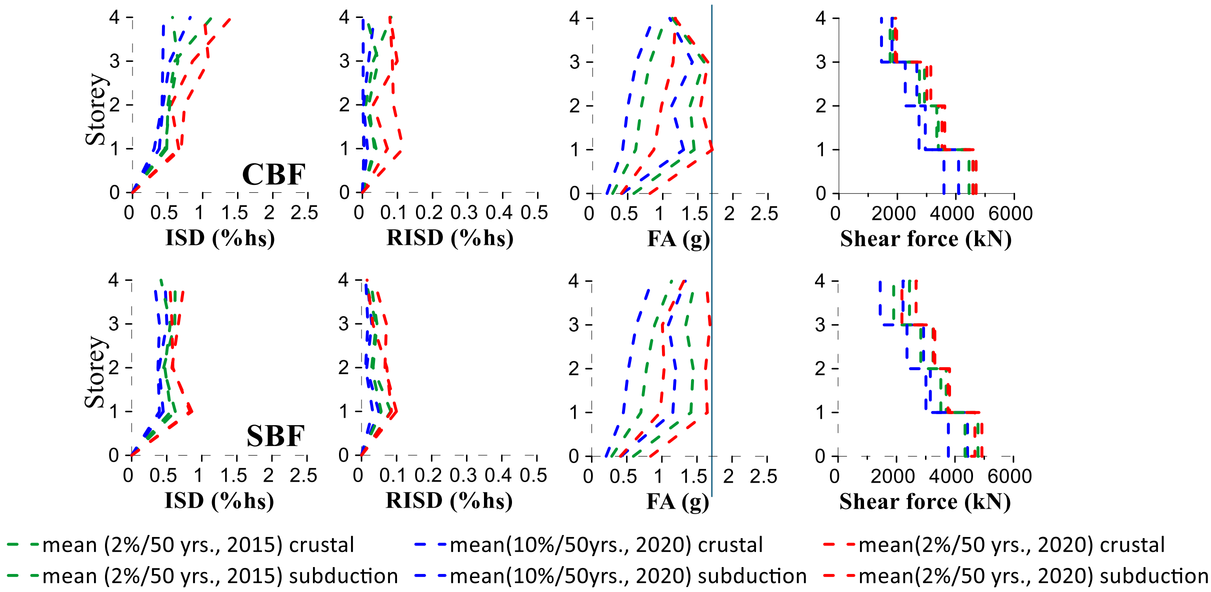

Fig. 7: Mean of key response parameters under crustal and subduction zone GMs scaled at different intensities.

Under 10%/50 yrs. design spectrum associated with [6], some damage could be exhibited by acceleration-sensitive nonstructural components under subduction GMs (blue lines in Fig. 7).

Figures 8 and 9 presents the incremental dynamic analysis (IDA) curves for the 4-storey MD-CBF and SBF building, respectively, under both crustal and subduction zone GMs. Herein, the black and red horizontal dashed line indicate the intensity demand at D.L. as per [7] and [6], respectively, while the blue horizontal dashed line as per [7] is added for discussion purposes. Key performance milestones are marked as follows: solid black circles denote the yielding of the first ductile brace (DB yields), and void circles denote the collapse point. In addition, black diamonds represent the failure of the first ductile brace, void diamonds indicate the failure of second ductile brace, black and void triangles signify the yielding of the first and second braces of SB truss, respectively, and black crosses mark the occurrence of RISD =0.5%h_s. Researchers [17] noted that damaged buildings with RISD ≥ 0.5%h_s are prone to demolition since the retrofit cost is greater than the replacement cost.

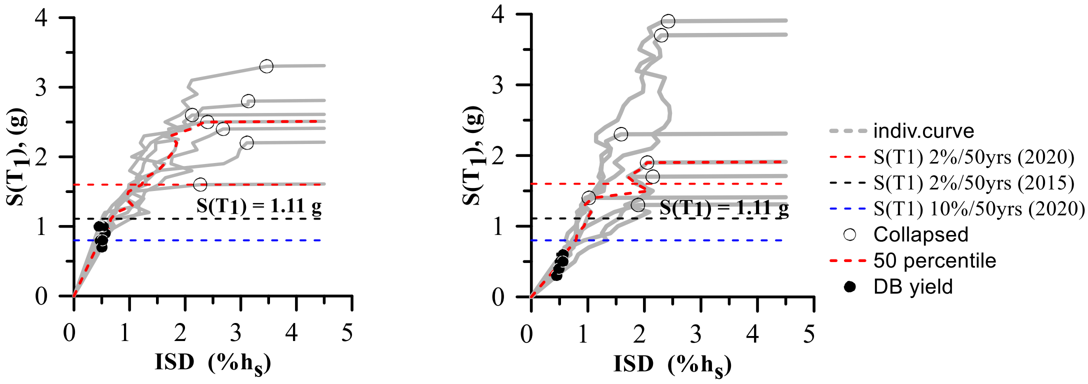

(a) (b)

Fig. 8: IDA curves of MD-CBF building under: a) crustal GMs and b) subduction zone GMs.

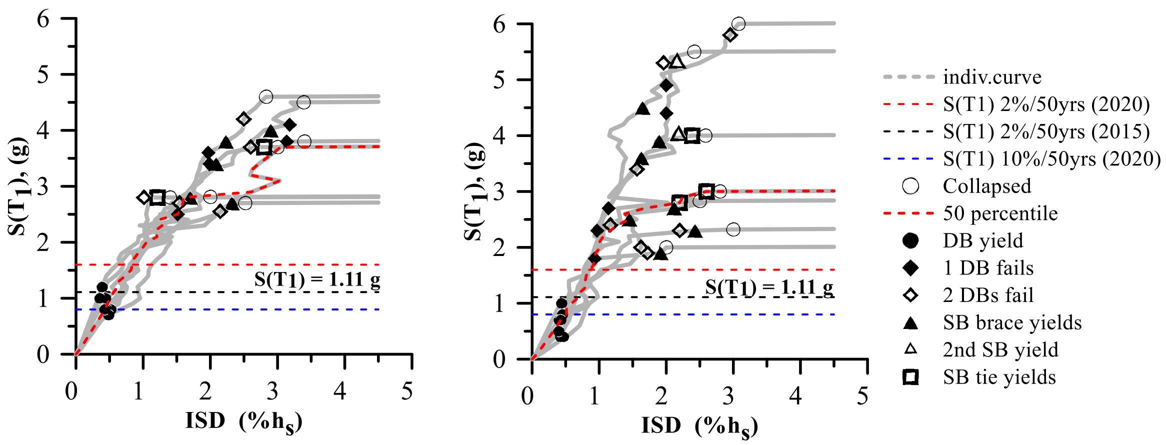

(a) (b)

Fig. 9: IDA curves of SBF building under: a) crustal GMs and b) subduction zone GMs.

From Figs. 8 and 9 result that ductile braces yield at lower intensity under subduction than crustal GMs. The MD-CBF building shows sufficient safety margin under crustal GMs and lower safety margin under subduction records, where it reached collapse under two GMs at an intensity slightly above D.L. as per [7]. Under subduction GMs, five IDA curves for the SBF building exhibit weaving behavior, and two IDAs under #S1 and #S3 GMs show softening behavior. Notably, the SBF building reached collapse capacity at higher intensity demands than the MD-CBF building; hence, the SBF showed the capability of mitigating the soft-storey response even after two ductile braces reached failure. From Fig. 9 results that the SBF of 4-

storey building can allow shelter in place under crustal ground motions associated with 10%/ 50 years earthquake. However, under 10/50 years subduction zone ground motions, at list one brace exhibited buckling. Thus, for recovery-based design, SBF with “damage-free” braces, as friction-sliding braces, are recommended.

4 CONCLUSIONS

To mitigate the concentration of damage under seismic excitations, the feasibility of SBF is presented through a case study in Victoria, B.C., where both crustal and subduction zone GMs are considered. The case study is a 4-storey office building braced by SBFs and for comparison purposes by MD-CBFs designed according with [7] and [12]. The SBF is composed of a primary ductile system derived from MD-CBF and an exterior elastic vertical truss (strongback) that is able to re-center the system and prevent the occurrence of dynamic instability. Although this system is not new, a comprehensive method used to size the strongback truss (SB) members was lacking. It is worth mentioning that higher modes forces developed in SBF are not limited by the yield mechanism of ductile system but by ground motion intensity, which implies large inertial effects relative to first-mode response. However, forces in the first mode are limited by the global mechanism.

At design level demand (2%/50 years) associated to [7], ductile braces reached buckling and several performed in nonlinear range under both crustal and subduction GMs, while the SB truss behaves elastically. Moreover, the nonlinear response of SBF in terms of ISD and RISD is not affected by the long duration subduction GMs, but floor accelerations and storey shear increase due to higher mode contribution. In addition, FAs induced by subduction GMs increase by more than 50% when comparing with FAs resulted under crustal GMs. Based on fragility curves provided in PACT library, FAs larger than 1.0 g imply damage to some acceleration-sensitive nonstructural components. Due to buckling of ductile braces at lower demand, both MD-CBF and SBF systems shall be retrofitted before allowing the shelter-in-place condition. However, using SBF with “free-damage” braces will allow shelter-in-place occupancy. It is noted that 2%/50 yrs. design spectrum provided in [7] is similar to 5%/50 yrs. acceleration response spectrum given in [6].

Under 10%/50 years demand associated to [6], buckling of first brace occurred under 3 out of 7 crustal GMs and under more than 50% subduction GMs. However, both MD-CBF and SBF responses in terms of ISD and FA do not imply damage to nonstructural components under crustal GMs, but some damage to acceleration-sensitive nonstructural components under subduction GMs. If ductile braces remain elastic, both MD-CBF and SBF buildings allow re-occupancy under crustal records.

From incremental dynamic analyses resulted that both 4-storey MD-CBF and SBF buildings pass the collapse safety criteria under crustal GMs. However, under subduction GMs excitation, the 4-storey MD-CBF exhibits borderline passing and the system is not recommended in subduction zone prone regions, while the SBF showed sufficient margin safety. Meanwhile, the SBF is able to exhibit lower RISD, even after one or two ductile braces experienced failure. This leads to the assurance of reparability criteria and feasibility of SBF system in high-risk seismic regions. Although the response of SBF to crustal GMs scaled at design level does not damage the nonstructural components, the subduction GMs may damage some acceleration-sensitive nonstructural components.

REFERENCES

[1] Federal Emergency Management Agency (FEMA), (2018 a), Seismic Performance Assessment of Buildings, Volume 1: Methodology (*FEMA P-58-1*), Washington, DC: FEMA, 2018.

[2] Federal Emergency Management Agency (FEMA), (2018, b), Seismic Performance Assessment of Buildings, Volume 3: Supporting Electronic Materials and Background Documentation (*FEMA P-58-3*), Washington, DC: FEMA, 2018.
[3] Terzic, V., Villanueva, PK, Saldana, D, Yoo, DY., (2021). F-Rec Framework: Novel Framework for probabilistic evaluation of functional recovery of building systems. *PEER Report* No. 2021/06.
[4] Almufti, I., Willford, M. (2013). Resilience-based earthquake design initiative (REDi™) for the next generation buildings. *ARUP*.
[5] NIST-FEMA (2020) Recommended options for improving the built environment for post-earthquake re-occupancy and functional recovery time, FEMA P-2090/NIST SP-1254, *Joint publication by FEMA and NIST*.
[6] National Research Council of Canada (2022): National Building Code of Canada (NBC 2020) Volume 1, Division B, Part 4, Structural Design, Edition 2020.
[7] National Research Council of Canada, National Building Code of Canada (ON), 2015.
[8] Chopra, A. K., Goel, R. K., & Chintanapakdee, C. (2004). Evaluation of a Modified MPA Procedure Assuming Higher Modes as Elastic to Estimate Seismic Demands. *Earthquake Spectra*, 20(3), 757–778.
[9] Wiebe, L., Sidwell, G. and Gledhill, S. (2015). Design guide for controlled rocking steel braced frames. Manukau city, New Zealand: *Steel Construction New Zealand*.
[10] Chen, L., Tremblay, R., Tirca, L. (2019). Practical seismic design procedure for steel braced frames with segmental elastic spines. *J. of Construct. Steel Research* 153, 395-415.
[11] Martin, R., & Deierlein, G. G. (2021). Generalized Modified Modal Superposition Procedure for Estimating Forces in Strongback Braced Frames. *J. of Struct. Eng.*, 147(5).
[12] Canadian Standards Assoc. (CSA), Design of steel structures, *S16:14 standard*, ON, 2014.
[13] Simson, B. (2020). Higher-mode force response in multi-story strongback-braced frames. *Earthquake Engng. Struct. Dyn.,* 49(14), pp.1406-1427, (2020).
[14] Lin, J.L., Kek, M.K., Tsai, K.C. (2019). Stiffness configuration of strongbacks to mitigate interstory drift concentration in buildings. *Eng. Structures* 199 (2019).
[15] Tirca, L., Chen, L., Tremblay, R. (2015). Assessing collapse safety of CBF buildings subjected to crustal and subduction earthquakes. *J. of construct. Steel Research*, 115,
[16] Shuaikang Wang (2024). The effects of ground motions characteristics and higher modes on the seismic response of steel Strongback Braced Frame buildings. M.A.S.c thesis, *Concordia University*, Montreal, Canada.
[17] McCornic, J., Aburano, H., Ikenaga, M., Nakashima, M., (2008). Permissible residual deformation levels for building structures considering both safety and human elements. P*roc. 14th World Conf. Earthquake Engineering,* Seismological press of China, Beijing.